ELSEVIER

Chemical Engineering Journal 117 (2006) 213–221

Chemical Engineering Journal

www.elsevier.com/locate/cej

Dynamic optimization of electrochemical reactors for the exact optimal control of consecutive electrochemical reactions

Vijayasekaran Boovaragavan [1], C. Ahmed Basha *

Central Electrochemical Research Institute, Karaikudi 630006, India

Received 17 May 2005; accepted 3 January 2006

Abstract

The kinetics, mass transfer, surface dynamics and double layer charging of consecutive electrochemical reactions have been investigated so as to set up a complete formulation and dynamic optimization of its performance in batch electrochemical reactors. The dynamic optimization problem statements are exclusively put together to represent the behavior of both Faradaic and non-Faradaic processes and consequently the formulated dynamic problems have been solved using the maximum principle. The results of applying the optimal time-varying profiles of electrode potential are compared between the two different modes of batch electrochemical reactor and also with those resulting from the tradition-operating style of these reactors. Despite the effect due to double layer charging, an enhanced selectivity result has been obtained even in the presence of significant mass transfer resistance by determining the best transient operating profile of control variable. Besides these, this paper also discusses on the methodology of dynamic optimization in continuous stirred tank and plug flow electrochemical reactors.

Keywords: Dynamic optimization; Electrochemical reactor; Optimal control; Series of reactions; Pontryagin maximum principle

1. Introduction

Electro-organic synthesis reactions have been extensively studied in the laboratory, but few are performed industrially; one typical problem is low reaction selectivity at the electrode potential necessary for commercial operation. As a means to improve reaction selectivity, Bakshi and Fedkiw [1] demonstrated theoretically the potential utility of optimal-control theory for a branched chemical-electrochemical reaction, which has not been extensively applied to electrochemical reactors although static optimization of electrochemical processes is keen and well-discussed topic [2]. Subsequently Fournier et al. [3] reported increased selectivity for the reduction of oxalic acid to glyoxalic acid; different dynamic optimization methods have been used for the determination of optimal time-varying profiles of electrode potential. Zhou et al. [4] studied the same process and demonstrated the methodology of using the K–L expansion in optimal control. A variational approach to the control of electrochemical hydrogen reactions was reported [5] for different cost objective and admissible control strategies. More recently, Vijayasekaran and Basha [6] explained the importance of surface concentration dynamics during process control policy evaluation by means of a coupled chemical-electrochemical reaction sequence using the calculus of variation.

Previous contributions on the optimization of batch electrochemical reactor for consecutive electrochemical reactions assumed steady state assumption for the exclusion of surface concentration variation during the batch time. This assumption is quite contradictory while doing the dynamic optimization. The effect of surface concentration on the reaction rate is of significant magnitude in many electrochemical processes. Moreover, the effect of non-Faradaic phenomena is also greatly ignored. In general non-Faradaic phenomena plays a very important role in time dependent variation of electrode potential and in particular, it predominates while starting-up the process. Therefore, while making up a control policy the knowledge of these should be taken into account for the successful design of optimal controller and also for an efficient online implementation of control strategy in batch electrochemical reactors.

When a current is applied to an electrode it becomes distributed among the processes of: (a) non-Faradaic – charging the double layer and charging the specific interactions between

* Corresponding author. Tel.: +91 4565 227550; fax: +91 4565 227779.
E-mail addresses: vijayasekaranb@yahoo.com (V. Boovaragavan), basha@cecri.res.in, cab_50@yahoo.co.in (C.A. Basha).
[1] Department of Chemical Engineering, Tennessee Technological University, Cookeville, TN 38505, USA.

1385-8947/$ – see front matter © 2006 Elsevier B.V. All rights reserved.
doi:10.1016/j.cej.2006.01.001

the electrode; and certain carriers (b) Faradaic – electron transfer reaction between the electrode and acceptors/donors in the solution and also mass transport as a result of coupling of these phenomena with bulk solution. The general equation for total current i_T as a function of electrode potential E, in the unsteady state form from which E as function of time t can be obtained is written as follow

$$i_T = C_{dl}\frac{dE}{dt} + q\frac{d\theta}{dt} + \sum_j r_j = (C_{dl} + C_\phi)\frac{dE}{dt} + \sum_j r_j \quad (1)$$

where C_{dl} is the double-layer capacitance; and q can be taken as the charge required for monolayer coverage of the adsorbed species; $-r_j$ is the rate of the jth electrochemical reaction; and C_ϕ (=qdθ/dE), the pseudocapacitance.

The first term in Eq. (1) represents the charge necessary to equalize the charge on the metal surface, i.e. the double layer charging. The study of electrical double layer is important because the charge distribution in a given system influences the electron transfer and thus the course of electrochemical reaction. In the double layer at plane electrodes, charge densities of about 16–50 $\mu F\,cm^{-2}$ are commonly realizable and so C_{dl} has certain effect on the electrode reaction rate. The second term represents the pseudocapacitance associated with chemisorbed electroactive intermediates in the electrode process and hence information on characteristics of the corresponding electrochemical isotherms. This pseudocapacitance behavior of the electrode interface bearing electroactive-chemisorbed intermediates is vital only in the case of high area porous electrode material used in electrochemical power sources [7]. In battery and fuel cells, this mechanism accommodates about 2–5% of the total charge accepted. In electrochemical capacitors, the charge storage process is totally non-Faradaic, i.e. ideally no electron transfer takes place across the electrode interface and the storage of electric charge and energy is electrostatic. But, in electrochemical synthesis, the charge for adsorption–desorption is much lesser than the double-layer electronic charge. Hence, in the subsequent sections it is taken that the total current is distributed among the rest of the phenomena.

The objective of the present work is to incorporate the surface concentration dynamics in batch reactor for consecutive electrochemical reactions together with the effect of double layer charging. To demonstrate the present methodology, the optimal time-varying electrode potential are determined for a potentially useful organic synthesis A ⇆ B ⇆ D (the electro reduction of oxalic acid to glyoxylic acid) taking place in a batch electrochemical reactor with and without electrolyte recirculation. The rest of the paper is organized as follows: the general dynamic optimization problem and the solution method are discussed first. This is followed by the formulation of dynamic optimization problem statement. Next, the computational results are discussed that provides a physical basis for the predicted trends. Finally, some generalizations are presented for the optimal control of continuous stirred tank electrochemical reactor (CSTER) and plug flow electrochemical reactor (PFER).

2. Mathematical analysis and computational method

Many physical systems are naturally described by differential-algebraic equations (DAEs). A general dynamic optimization problem can be written as

$$\text{Maximize } I = \int_0^{t_f} \chi(\boldsymbol{x}, \boldsymbol{u}, t)\,dt \quad (2a)$$

Subject to

$$\boldsymbol{f}(\dot{\boldsymbol{x}}, \boldsymbol{x}, \boldsymbol{u}, t) = 0 \quad (2b)$$

$$\boldsymbol{g}(\boldsymbol{x}, \boldsymbol{u}, t) = 0 \quad (2c)$$

$$\boldsymbol{h}(\boldsymbol{x}, \boldsymbol{u}, t) \le 0 \quad (2d)$$

where (2c) are addition equality constraints and (2d) are additional inequality constraints. $\boldsymbol{x}$ is a vector of state variables x_1, $x_2, \ldots, x_n$; and $\boldsymbol{u}$, a vector of control variables $u_1, u_2, \ldots, u_r$. In our cases, there is only one additional equality constraint; the constraint is accounted for by the use of Lagrange multiplier λ, combining Eqs. (2a) and (2c),

$$\bar{I} = \int_0^{t_f} [\chi(\boldsymbol{x}, \boldsymbol{u}, t) - \lambda \boldsymbol{g}(\boldsymbol{x}, \boldsymbol{u}, t)]\,dt \quad (3)$$

Now, instead of I, $\bar{I}$ should be maximized. To solve this problem, an additional state variable $x_i(t)$ is introduced. It follows then, that

$$\dot{x}_{n+1} = [\chi(\boldsymbol{x}, \boldsymbol{u}, t) - \lambda \boldsymbol{g}(\boldsymbol{x}, \boldsymbol{u}, t)]; \quad x_{n+1}(0) = 0 \quad (4)$$

The problem is thus transformed into one of maximizing $x_{n+1}(t_f)$ for a DAEs system described by Eqs. (2b) and (4). Now, the variational problem of interest is, to maximize an integral functional

$$J_0 = J_0[x_{n+1}(t_f)] \quad (5)$$

subject to the constraints

$$\dot{\boldsymbol{x}} = \boldsymbol{f}(\boldsymbol{x}(t), \boldsymbol{u}(t)); \quad \boldsymbol{x}(0) = \boldsymbol{x}_0 \quad (6a)$$

$$\dot{x}_{n+1} = [\chi(\boldsymbol{x}, \boldsymbol{u}, t) - \lambda \boldsymbol{g}(\boldsymbol{x}, \boldsymbol{u}, t)]; \quad x_{n+1}(0) = 0 \quad (6b)$$

The above-constrained optimization problem can be transformed into a non-constrained optimization problem by defining an augmented performance index.

$$J = J_0 + \int_0^{t_f} \sum_{i=1}^{n+1} \gamma_i \left[-\dot{\boldsymbol{x}}_i + f_i(\boldsymbol{x}(t), \boldsymbol{u}(t))\right] dt \quad (7)$$

where γ_i's are the Lagrange multipliers: they are determined optimally by the computational method used. The resulting problem Eq. (7) is then a standard unconstrained optimization problem whose solution, if it exists, satisfies the following differential-algebraic system [8].

At this stage, it is convenient to introduce a new function H called 'Hamiltonian' which is defined as

$$H = \sum_{i=1}^{n+1} \gamma_i f_i(\boldsymbol{x}(t), \boldsymbol{u}(t)) \quad (8)$$

with the help of H, we can write the differential-algebraic system equations as

$$\dot{\boldsymbol{x}} = \frac{\partial H}{\partial \gamma}, \quad \boldsymbol{x}(0) = \boldsymbol{x}_0 \tag{9a}$$

$$\dot{\gamma} = -\frac{\partial H}{\partial \boldsymbol{x}}, \quad \gamma(t_\mathrm{f}) = \left[\frac{\partial J_0}{\partial \boldsymbol{x}}\right]_{t_\mathrm{f}} \tag{9b}$$

$$\frac{\partial H}{\partial \mathbf{u}} = 0 \tag{9c}$$

It can be seen that the resulting DAEs system is a two-point boundary value problem that require numerical procedures. Therefore, the computational procedure as outlined in Fig. 1 is followed. Optimal control profiles under different conditions are determined by using one of the major mathematical functional areas of Maple® 8.00 by Waterloo Maple Inc., the differential equations.

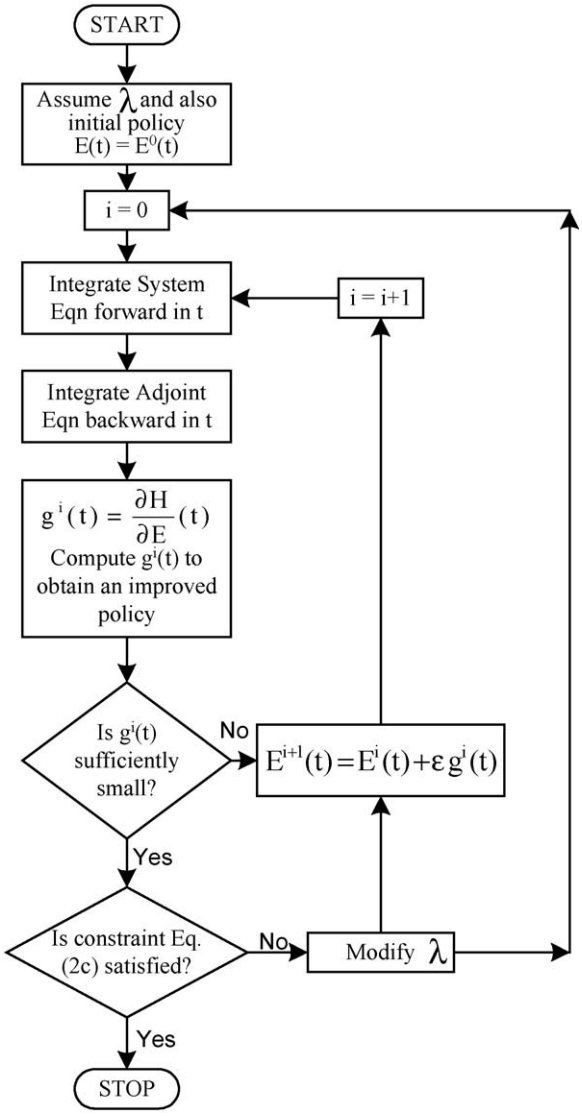

Fig. 1. Algorithm used for computing optimal control profile.

3. Batch electrochemical reactor

The consecutive electrochemical reactions under consideration is similar to the electrochemical reduction of the reactant oxalic acid (A) to a desired product glyoxalic acid (B) and further electrochemical reduction to the by-product glycolic acid (D) as $A \overset{n_1 e^-}{\longleftrightarrow} B \overset{n_2 e^-}{\longleftrightarrow} D$. The schematic of various electrochemical reactors used for dynamic modeling are presented in Fig. 2. The dynamics of reactants and various electrochemical products over the surface of an electrode and in the bulk is usually modeled [9] through a combination of electrochemical reaction and mass transport velocities. The component material balances for each species are

$$\frac{\mathrm{d}C_\mathrm{A}^\mathrm{b}}{\mathrm{d}t} = -k_{\mathrm{L_A}} a (C_\mathrm{A}^\mathrm{b} - C_\mathrm{A}^\mathrm{s}) \tag{10a}$$

$$\frac{\mathrm{d}C_\mathrm{A}^\mathrm{s}}{\mathrm{d}t} = k_{\mathrm{L_A}} a (C_\mathrm{A}^\mathrm{b} - C_\mathrm{A}^\mathrm{s}) - k_{\mathrm{fl}_0} a e^{-\alpha_1 fE} C_\mathrm{A}^\mathrm{s} + k_{\mathrm{bl}_0} a e^{-\beta_1 fE} C_\mathrm{B}^\mathrm{s} \tag{10b}$$

$$\frac{\mathrm{d}C_\mathrm{B}^\mathrm{b}}{\mathrm{d}t} = k_{\mathrm{L_B}} a (C_\mathrm{B}^\mathrm{s} - C_\mathrm{B}^\mathrm{b}) \tag{10c}$$

$$\frac{\mathrm{d}C_\mathrm{B}^\mathrm{s}}{\mathrm{d}t} = -k_{\mathrm{L_B}} a (C_\mathrm{B}^\mathrm{s} - C_\mathrm{B}^\mathrm{b}) + k_{\mathrm{fl}_0} a e^{-\alpha_1 fE} C_\mathrm{A}^\mathrm{s} - k_{\mathrm{bl}_0} a e^{-\beta_1 fE} C_\mathrm{B}^\mathrm{s} - k_{\mathrm{f2}_0} a e^{-\alpha_2 fE} C_\mathrm{B}^\mathrm{s} + k_{\mathrm{b2}_0} a e^{-\beta_2 fE} C_\mathrm{D}^\mathrm{s} \tag{10d}$$

$$\frac{\mathrm{d}C_\mathrm{D}^\mathrm{b}}{\mathrm{d}t} = k_{\mathrm{L_D}} a (C_\mathrm{D}^\mathrm{s} - C_\mathrm{D}^\mathrm{b}) \tag{10e}$$

$$\frac{\mathrm{d}C_\mathrm{D}^\mathrm{s}}{\mathrm{d}t} = -k_{\mathrm{L_D}} a (C_\mathrm{D}^\mathrm{s} - C_\mathrm{D}^\mathrm{b}) + k_{\mathrm{f2}_0} a e^{-\alpha_2 fE} C_\mathrm{B}^\mathrm{s} - k_{\mathrm{b2}_0} a e^{-\beta_2 fE} C_\mathrm{D}^\mathrm{s} \tag{10f}$$

Here, C_i^b is the bulk concentration of the species i; C_i^s, the concentration at the electrode surface; k_{L_i}, the mass transfer coefficient of species i; $f = F/RT$; α and β are the transfer coefficients; and 'a', the specific electrode area. The total current is expressed as a sum of Faradaic and non-Faradaic current as

$$i_\mathrm{T} = C_\mathrm{dl}\frac{\mathrm{d}E}{\mathrm{d}t} + n_1 F(k_{\mathrm{f1}} C_\mathrm{A}^\mathrm{s} - k_{\mathrm{b1}} C_\mathrm{B}^\mathrm{s}) + n_2 F(k_{\mathrm{f2}} C_\mathrm{B}^\mathrm{s} - k_{\mathrm{b2}} C_\mathrm{D}^\mathrm{s}) \tag{11}$$

Thus, the problem can be stated as

$$\text{Maximize } I = \int_0^{t_\mathrm{f}} C_\mathrm{B}^\mathrm{b}(t)\,\mathrm{d}t \tag{12}$$

subject to the differential constraints Eqs. (10a)–10(f) and an additional equality constraint Eq. (11). The dimensionless forms of these equations are useful to define the problem more closely.

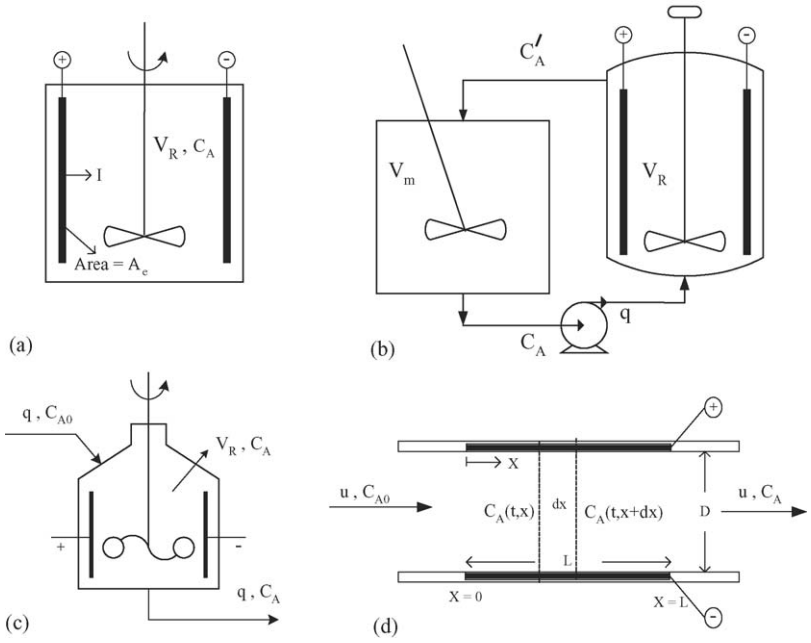

Fig. 2. Schematic representation of the batch and continuous flow electrochemical reactors. (a) Batch electrochemical reactor; (b) batch electrochemical reactor with electrolyte recirculation; (c) continuous stirred tank electrochemical reactor (CSTER); (d) plug flow electrochemical reactor (PFER).

$$\tau_1^* = \frac{t_f}{V_m/q}; \quad \tau_2^* = \frac{t_f}{V_R/q}; \quad t^* = \frac{t}{t_f}; \quad x_i = \frac{C_i}{C_{A_0}}$$
$$i_T^* = \frac{i_T}{nF}\frac{at_f}{C_{A_0}}; \quad C_{dl}^* = \frac{at_f}{nFC_{A_0}}C_{dl} \tag{13}$$
$$k_{L_i}^* = k_{L_i} at_f; \quad i = A, B \,\&\, D$$
$$k_{f_i}^* = k_{fi_0} at_f e^{-\alpha_i fE} \,\&\, k_{b_i}^* = k_{bi_0}\, at_f e^{-\beta_i fE}; \quad i = 1, 2$$

Introducing these dimensionless quantities in to the governing model equations, the dynamic optimization problem statement can be written as follow:

$$\text{Maximize } I = x_3(1) \tag{14}$$

such that

$$\dot{x}_1 = -k_{L_A}^*(x_1 - x_2) \tag{15a}$$
$$\dot{x}_2 = k_{L_A}^*(x_1 - x_2) - k_{f1}^* x_2 + k_{b1}^* x_4 \tag{15b}$$
$$\dot{x}_3 = k_{L_B}^*(x_4 - x_3) \tag{15c}$$
$$\dot{x}_4 = -k_{L_B}^*(x_4 - x_3) + k_{f1}^* x_2 - k_{b1}^* x_4 - k_{f2}^* x_4 + k_{b2}^* x_6 \tag{15d}$$
$$\dot{x}_5 = k_{L_D}^*(x_6 - x_5) \tag{15e}$$
$$\dot{x}_6 = -k_{L_D}^*(x_6 - x_5) + k_{f2}^* x_4 - k_{b2}^* x_6 \tag{15f}$$
$$\text{and } i_T^* = C_{dl}^* \dot{E}^* + k_{f1}^* x_2 + (k_{f2}^* - k_{b1}^*)x_4 - k_{b2}^* x_6 \tag{16}$$

Only reactant A is present initially, which results in the initial conditions

$$x_1(0) = 1.0 \tag{17a}$$
$$x_i(0) = 0 \quad \text{where } i = 2, 3, ..., 6 \tag{17b}$$

As discussed in Section 2, in applying the numerical procedure shown in Fig. 1, it is necessary to introduce a seventh state variable $x_7(t)$, defined as

$$x_7(t^*) = \int_0^1 x_3 - \lambda[C_{dl}^* \dot{E}^* + k_{f1}^* x_2 + (k_{f2}^* - k_{b1}^*)x_4 - k_{b2}^* x_6 - i_T^*]\, dt^* \tag{18}$$

Then it follows,

$$\dot{x}_7 = x_3 - \lambda \left\lfloor C_{dl}^* \dot{E}^* + k_{f1}^* x_2 + (k_{f2}^* - k_{b1}^*)x_4 - k_{b2}^* x_6 - i_T^* \right\rfloor;$$
$$x_7(0) = 0 \tag{19}$$

The problem is now transformed into one of maximizing $J_0 = J_0[x_7(t)]$ (ref. Eq. (5)) for a system described by Eqs. (15a)–(15f) and (19) by a proper choice of $E(t)$, $0 \le t \ge t_f$. At correct value of λ, $x_7(t)$ becomes equal to I, Eq. (14). The derivative of the Hamiltonian for this system is,

$$\frac{\partial H}{\partial E^*} = k_{f1}^* \alpha_1 x_2(\gamma_2 - \gamma_4 + \lambda\gamma_7) - k_{f2}^* \alpha_2 x_4(\gamma_4 - \gamma_6 + \lambda\gamma_7) \tag{20}$$

The corresponding adjoint equations are derived as follows:

$$\dot{\gamma}_1 = k_{L_A}^*(\gamma_1 - \gamma_2) \tag{21a}$$
$$\dot{\gamma}_2 = -k_{L_A}^* \gamma_1 + (k_{L_A}^* + k_{f_1}^*)\gamma_2 - k_{f_1}^* \gamma_4 + \lambda k_{f_1}^* \gamma_7 \tag{21b}$$
$$\dot{\gamma}_3 = k_{mB}^*(\gamma_3 - \gamma_4) \tag{21c}$$
$$\dot{\gamma}_4 = -k_{b_1}^* \gamma_2 - k_{L_B}^* \gamma_3 + (k_{L_B}^* + k_{b_1}^* + k_{f_2}^*)\gamma_4 - k_{f_2}^* \gamma_6 + \lambda(k_{f_2}^* - k_{b_1}^*)\gamma_7 \tag{21d}$$
$$\dot{\gamma}_5 = k_{mE}^*(\gamma_5 - \gamma_6) \tag{21e}$$
$$\dot{\gamma}_6 = -k_{b_2}^* \gamma_4 + (k_{mE}^* + k_{b_2}^*)\gamma_6 - k_{mE}^* \gamma_5 \tag{21f}$$

$$\dot{\gamma}_7 = 0 \tag{21g}$$

With boundary conditions

$$\gamma_i(1) = 0 \quad \text{where } i = 1, 2, ..., 6 \text{ and } \gamma_7(1) = 1.0 \tag{22}$$

The boundary conditions in Eq. (22) are derived from Eq. (9b). The control variable $E(t)$ can be expressed in terms of state and adjoint variables as

$$E(t) = \frac{1}{(\alpha_2 - \alpha_1)f} \ln\left[\frac{\alpha_2 k_{f2_0} x_4(\gamma_6 - \gamma_4 - \lambda\gamma_7)}{\alpha_1 k_{f1_0} x_2(\gamma_2 - \gamma_4 + \lambda\gamma_7)}\right] \tag{23}$$

Integrating last of Eqs. (21a)–(21g), one obtains $\gamma_7(t) = 1$; hence, this adjoint equation drops out. Starting with assumed values for control policy $E^0(t)$ and λ, the procedure as in Fig. 1 has been followed for computation of optimal $E(t)$. The state equations are solved using the initial value problem (IVP) solver and the adjoint equations using the boundary value problem (BVP) solver. For a particular iteration, the Maple's dsolve command performs this evaluation. The type of problem (BVP or IVP) is automatically detected by dsolve, and the appropriate method is used. The default IVP method is a Runge-Kutta Fehlberg method, which produces a solution accurate to fifth order. The trapezoid method is generally used for typical BVP problems. The physical data used for the computation are as follow: $a = 140.1\ \text{m}^{-1}$, $k_{mA} = 10^{-4}\ \text{ms}^{-1}$, $k_{mA}/k_{mB} = 10$, $k_{f10} = 10^{-13}\ \text{ms}^{-1}$, $k_{f20} = K_{f10}/3$, $k_{b10} = k_{b20} = 0$, $\tau_1 = 104.58$, $\tau_2 = 167.33$, $\alpha_1 = 0.162$, $\alpha_2 = 0.157$, $\beta_1 = \beta_2 = 0$, $T = 293.15\ \text{K}$.

Fig. 3a shows the best optimal time-varying potential profile for different mass transfer rates. As it can be seen that at very low times the potential to be applied is close to the upper limit of the control variable. As time increases, the potential decreases restricting the formation of undesired product. This is true because the formation of most of the desired electrochemical product and also double layer charging are taking place at the early stage of the reaction. Fournier et al. [3] have presented an optimal control policy for this reaction system, taking place in a batch electrochemical reactor without electrolyte recirculation. Using the different computation techniques, similar optimal electrode potential-time profile was obtained by Zhou et al. [4]. It can be noticed here (Fig. 3a) that for the same operating conditions the profile obtained is almost nearer the upper limit of the potential. Since they correspond to energy efficiency of the electrochemical process, the evaluated control policy has an industrial interest from the process economics point of view and thus necessitates electrolyte recirculation. Also, it can be observed that at kinetic-controlled conditions ($k_m = 10^{-4}\ \text{ms}^{-1}$) the potentials for time-varying control are smallest. It shows the importance of taking into account the surface concentration dynamics and non-Faradaic process at the optimization problem statement level and hence the importance of current efficiency.

Fig. 4a and b are the resultant concentration profiles over the batch period for the optimal time-varying potential control and static control, respectively. The best steady potential was found by solving numerically IVP Eqs. (15a)–(15f) using dsolve command for potentials differing by 0.01 V from −1.0 to −1.7 V and locating that corresponding to the maximum $x_3(t)$. Regardless of the value of k_m, the maximum production of the desired compound is obtained by the optimal control of the potential. The production rate provided by steady control further decreases as the mass transfer resistance increases because of the diminished sensitivity of the reaction rate to the applied constant potential. With optimal control, however, the percentage increase in the production and selectivity above the steady-control value increase with decreasing k_m. This interesting result is caused by the use of a short time high potential, i.e. during the start up and the gradual decrease in the applied potential. In this manner, mass transfer limitations are not as significant since the desired electrochemical reaction is not occurring for the majority of the time after this initial period. During the delayed time, the potential contribution for double layer charging is also helpful in preventing the undesired electrochemical reactions. Certainly, the production rate of the desired product B is high for all the

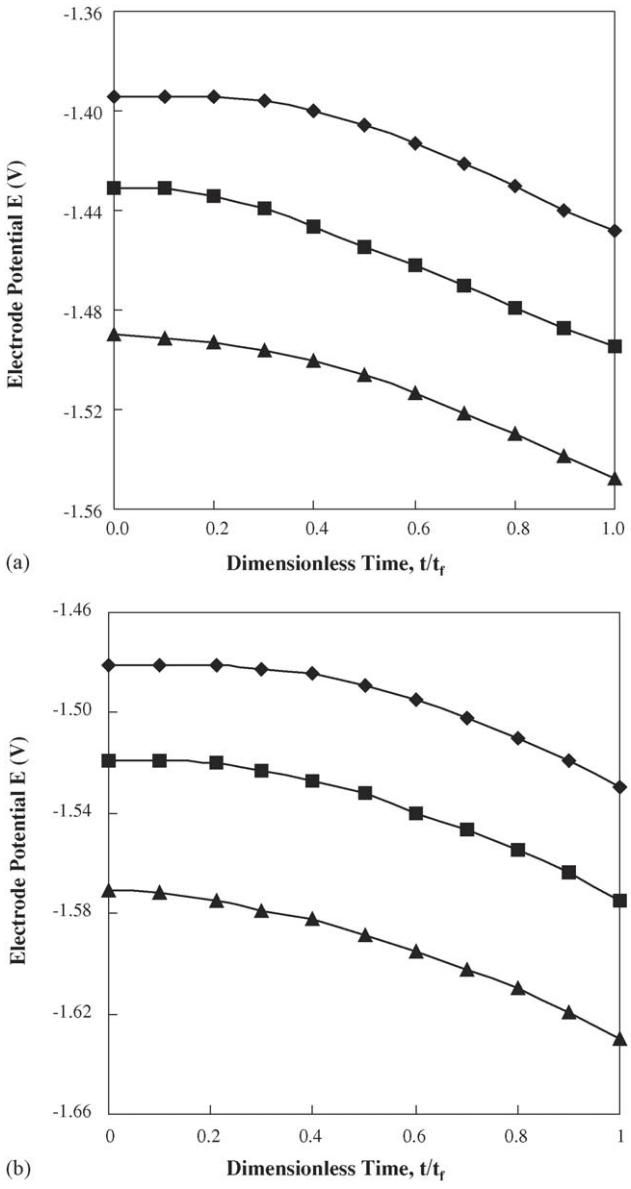

Fig. 3. Plots of optimal control profile for: (a) batch electrochemical reactor; (b) batch electrochemical reactor with electrolyte recirculation. (♦) Represents $k_m = 5 \times 10^{-5}\ \text{ms}^{-1}$, (■) $k_m = 7 \times 10^{-5}\ \text{ms}^{-1}$, (▲) $k_m = 10^{-4}\ \text{ms}^{-1}$.

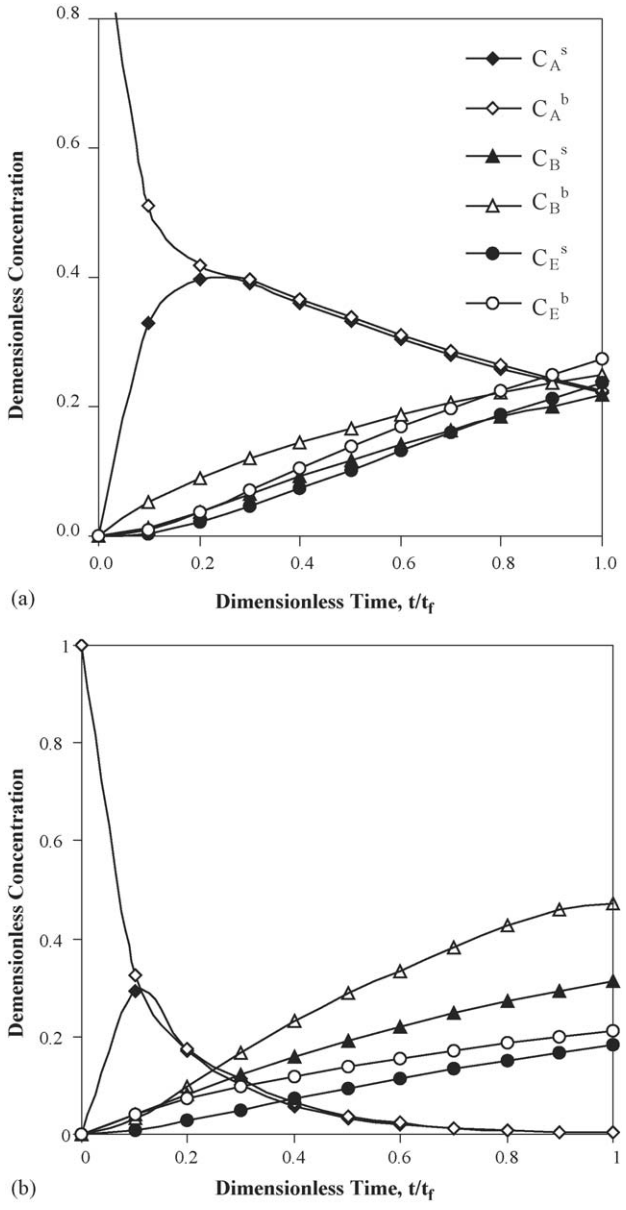

Fig. 4. Variation of dimensionless concentration on applying the: (a) best steady potential; and (b) optimal time-varying potential in batch electrochemical reactor.

three mass transfer limits, but percentage increase in the production above the steady control value decreases with increasing mass transfer resistance. An effort to overcome this trend is the use of electrolyte recirculation through a mixing tank and it is discussed in the next section.

4. Batch electrochemical reactor with electrolyte recirculation

The traditional concept of a batch reactor is that of a sealed vessel, in which no material is supplied or withdrawn and where the reaction is allowed to run its course (Fig. 2a). An application of this, seen later, is when batch electrochemical reactors are operated with a high degree of recycle. In electrosynthesis on an industrial scale, it is not always desirable to operate in these ways. Therefore, an alternative batch operation is realized, where a rapid recirculation of electrolyte from a mixing tank to a reactor, external to the tank, is achieved (Fig. 2b). The dynamic problem for this type of reactor has been formulated in the same way as accomplished for the batch electrochemical reactor. The model equations are

$$V_m \frac{dC_A}{dt} = qC'_A - qC_A \tag{24a}$$

$$V_R \frac{dC'_A}{dt} = -k_{L_A} A_e (C'_A - C^s_A) + qC_A - qC'_A \tag{24b}$$

$$\frac{dC^s_A}{dt} = k_{L_A} a (C'_A - C^s_A) - k_{f1_0} a e^{-\alpha_1 fE} C^s_A + k_{b1_0} a e^{-\beta_1 fE} C^s_B \tag{24c}$$

$$V_m \frac{dC_B}{dt} = qC'_B - qC_B \tag{24d}$$

$$V_R \frac{dC'_B}{dt} = -k_{L_B} A_e (C^s_B - C'_B) + qC_B - qC'_B \tag{24e}$$

$$\frac{dC^s_B}{dt} = -k_{L_B} a (C^s_B - C'_B) + k_{f1_0} a e^{-\alpha_1 fE} C^s_A - k_{b1_0} a e^{-\beta_1 fE} C^s_B - k_{f2_0} a e^{-\alpha_2 fE} C^s_B + k_{b2_0} a e^{-\beta_2 fE} C^s_D \tag{24f}$$

$$V_m \frac{dC_D}{dt} = qC'_D - qC_D \tag{24g}$$

$$V_R \frac{dC'_D}{dt} = -k_{L_D} A_e (C^s_D - C'_D) + qC_D - qC'_D \tag{24h}$$

$$\frac{dC^s_D}{dt} = -k_{L_D} a (C^s_D - C'_D) + k_{f2_0} a e^{-\alpha_2 fE} C^s_B - k_{b2_0} a e^{-\beta_2 fE} C^s_D \tag{24i}$$

The total current expression is same as given by Eq. (11) and the performance index is

$$\text{Maximize } I = \int_0^{t_f} C'_B(t)\, dt \tag{25}$$

The complete problem statement in dimensionless form is as follow:

$$\text{Maximize } I = x_5(1) \tag{26}$$

such that

$$\dot{x}_1 = \tau^*_1 (x_2 - x_1) \tag{27a}$$

$$\dot{x}_2 = -k^*_{L_A} (x_2 - x_3) + \tau^*_2 (x_1 - x_2) \tag{27b}$$

$$\dot{x}_3 = k^*_{L_A} (x_2 - x_3) - k^*_{f1} x_3 + k^*_{b1} x_6 \tag{27c}$$

$$\dot{x}_4 = \tau^*_1 (x_5 - x_4) \tag{27d}$$

$$\dot{x}_5 = k^*_{L_B} (x_6 - x_5) + \tau^*_2 (x_4 - x_5) \tag{27e}$$

$$\dot{x}_6 = -k^*_{L_B} (x_6 - x_5) + k^*_{f1} x_3 - k^*_{b1} x_6 - k^*_{f2} x_6 + k^*_{b2} x_9 \tag{27f}$$

$$\dot{x}_7 = \tau^*_1 (x_8 - x_7) \tag{27g}$$

$$\dot{x}_8 = k^*_{L_D}(x_9 - x_8) + \tau^*_2(x_7 - x_8) \quad (27h)$$

$$\dot{x}_9 = -k^*_{L_D}(x_9 - x_8) + k^*_{f2}x_6 - k^*_{b2}x_9 \quad (27i)$$

$$\text{and } i^*_T = C^*_{dl}\dot{E}^* + k^*_{f1}x_2 + (k^*_{f2} - k^*_{b1})x_4 - k^*_{b2}x_6 \quad (28)$$

The initial conditions for the state variables are

$$x_1(0) = 1.0 \quad (29a)$$

$$x_i(0) = 0 \quad \text{where } i = 2, 3, ..., 9 \quad (29b)$$

The problem is modified by taking into account the additional equality constraint Eqs. (27a)–(27i) by incorporating a state variable as

$$\dot{x}_{10} = x_5 - \lambda\left[C^*_{dl}\dot{E}^* + k^*_{f1}x_3 + (k^*_{f2} - k^*_{b1})x_6 - k^*_{b2}x_9 - i^*_T\right]; \quad x_{10}(0) = 0 \quad (30)$$

and the corresponding Hamiltonian derivative is,

$$\frac{\partial H}{\partial E^*} = k^*_{f1}\alpha_1 x_3(\gamma_3 - \gamma_6 + \lambda\gamma_{10}) - k^*_{f2}\alpha_2 x_6(\gamma_6 - \gamma_9 + \lambda\gamma_{10}) \quad (31)$$

The adjoint equations are

$$\dot{\gamma}_1 = \tau^*_1\gamma_1 - \tau^*_2\gamma_2 \quad (32a)$$

$$\dot{\gamma}_2 = -\tau^*_1\gamma_1 + (k^*_{L_A} + \tau^*_2)\gamma_2 - k^*_{L_A}\gamma_3 \quad (32b)$$

$$\dot{\gamma}_3 = -k^*_{L_A}\gamma_2 + (k^*_{L_A} + k^*_{f_1})\gamma_3 - k^*_{f_1}\gamma_6 + \lambda k^*_{f_1}\gamma_{10} \quad (32c)$$

$$\dot{\gamma}_4 = \tau^*_1\gamma_4 - \tau^*_2\gamma_5 \quad (32d)$$

$$\dot{\gamma}_5 = -\tau^*_1\gamma_4 + (k^*_{L_B} + \tau^*_2)\gamma_5 - k^*_{L_B}\gamma_6 - \gamma_{10} \quad (32e)$$

$$\dot{\gamma}_6 = -k^*_{b_1}\gamma_3 - k^*_{L_B}\gamma_5 + (k^*_{L_B} + k^*_{b_1} + k^*_{f_2})\gamma_6 - k^*_{f_2}\gamma_9 + \lambda(k^*_{f_2} - k^*_{b_1})\gamma_{10} \quad (32f)$$

$$\dot{\gamma}_7 = \tau^*_1\gamma_7 - \tau^*_2\gamma_8 \quad (32g)$$

$$\dot{\gamma}_8 = -\tau^*_1\gamma_7 + (k^*_{L_D} + \tau^*_2)\gamma_8 - k^*_{L_D}\gamma_9 \quad (32h)$$

$$\dot{\gamma}_9 = -k^*_{b_2}\gamma_6 - k^*_{L_D}\gamma_8 + (k^*_{L_D} + k^*_{b_2})\gamma_9 - \lambda k^*_{b_2}\gamma_{10} \quad (32i)$$

$$\dot{\gamma}_{10} = 0 \quad (32j)$$

with boundary conditions

$$\gamma_i(1) = 0 \quad \text{where } i = 1, 2, ..., 9 \text{ and } \gamma_{10}(1) = 1.0 \quad (33)$$

and the control variable in terms of state and adjoint variables is

$$E(t) = \frac{1}{(\alpha_2 - \alpha_1)f}\ln\left[\frac{\alpha_2 k_{f2_0}x_6(\gamma_9 - \gamma_6 - \lambda\gamma_{10})}{\alpha_1 k_{f1_0}x_3(\gamma_3 - \gamma_6 + \lambda\gamma_{10})}\right] \quad (34)$$

Thus, the system dynamics equations, which define the process, are given by Eqs. (27a)–(27i), (30) and (32a)–(32j). Two points on the extremum curve are fixed with the initial and boundary conditions (Eqs. (29a), (29b) and (33)) on the state and adjoint variable, respectively. The Hamiltonian derivative with respect to the control variable is given by Eq. (31), to improve the assumed profile. To aid in computation the control variable is also expressed in terms of the unknown variables by Eq. (34).

Computations are performed by invoking the dsolve function option numeric or type = numeric to find a numerical solution for the ODE system. In this case that an initial solution profile was not provided, the first error message indicates that dsolve/numeric cannot find a suitable initial solution profile. The second message indicates that the Newton iteration is not converging, because the provided solution profile is too different from the true solution. This is a difficult problem. Often this error arises when a problem has narrow boundary layers or sharp corner layers. The error messages suggest the best strategy for solving this problem is use of a different continuation or a finer mesh, but a greater number of initial points by using the initmesh argument. Thus, default integration properties of the ODEs solver performance are altered to overcome the convergence difficulties. But, this will not affect the main results.

Fig. 3b presents the optimal electrode potential-time profiles obtained by the above computational procedure. It is interesting to notice that the computation of optimal profiles of electrode potential is almost the same for both the reactor systems. It is therefore important to analyze how the attained performance index differs in these two systems. Fig. 5a and b compares the concentrations of the reactant and products during the batch time for the two modes of controlling the batch electrochemical process with electrolyte recirculation. To recognize the enhanced mass transport of species to and from an active electrode surface, these results should also be compared with the results of batch electrochemical reactor without electrolyte recirculation. It can be seen that the best production of the desired compound is obtained by the batch reactor with recirculation through a reservoir followed in order by the best time-varying electrode potential of batch reactor and static potential control of reactor with recirculation. Thus, using almost the same optimal control policy the production obtained for the case of batch with recirculation is considerably more than that of without recirculation of electrolyte. This significant improvement in productivity is caused due to the reactor system configuration that keeps the electrolyte majority of the batch time in the reservoir. It results in the restriction of undesired electrochemical reduction due to less electrochemical reaction time, but with maximum reactant depletion that would obviously results in maximum B. In contrast, under batch electrochemical reactor without recirculation the control of undesired product formation depends entirely on the optimal control policy. It is not aided by the reactor system configuration and electrode–electrolyte contact pattern.

Unlike chemical kinetics a direct control over the reaction velocities is attainable only in electrochemical reactions. This can be best achieved by the use of time-varying electrode potential, even though the analogous optimum temperature progression in chemical reactor can have some control over reaction rate. In contrast to chemical reactors, the dynamic manipulation of voltage or current is much easier than temperature (or concentration, flow rate, pressure, etc.) and offers intriguing possibilities for reaction engineering. The optimal, time-varying control of potential or current can be used to achieve objectives other than maximizing productivity; for example, the current efficiency or

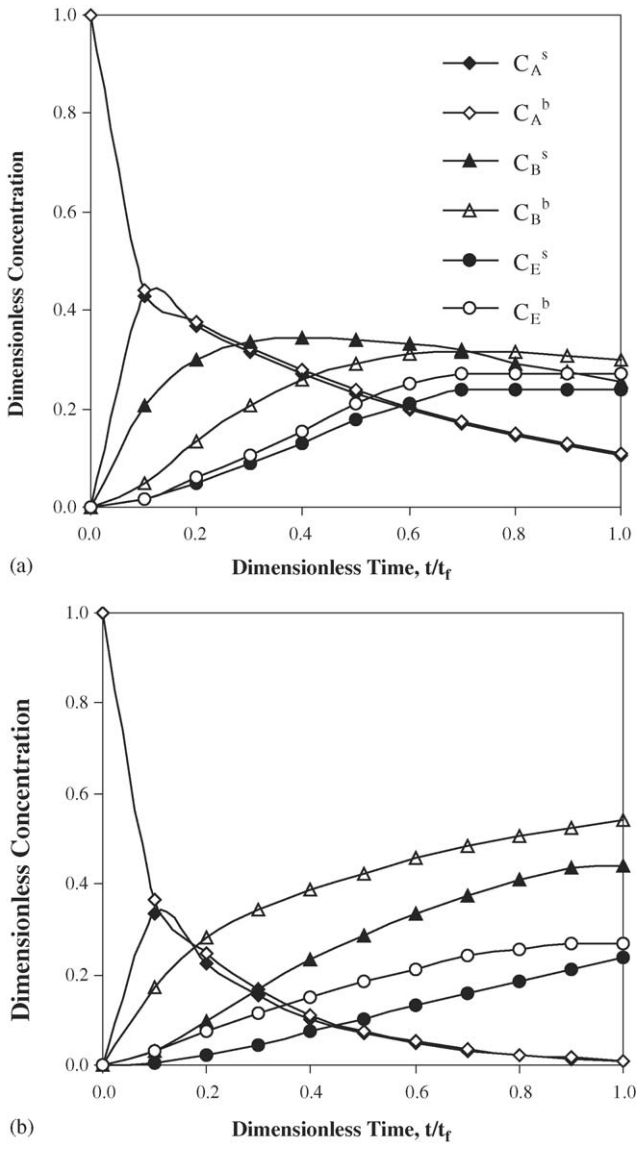

Fig. 5. Variation of dimensionless concentration on applying the: (a) best steady potential; and (b) optimal time-varying potential in batch electrochemical reactor.

selectivity can be maximized. Fig. 6 illustrates the qualitative nature of the reaction velocities for the consecutive electrochemical reaction scheme under kinetic control.

Thus, in the above investigation, the surface concentration changes during the electrochemical process with the correct objective function are accounted together with double layer effect. Optimal profiles of the electrode potential are accordingly realistic since the most important physical constraints are considered. The simple mathematical analysis described above can be carried out for other reactor systems to determine the best reactor configuration for a given reaction system. If an electrochemical reactor configuration is described for the consecutive electrochemical reactions, then the objective functional has to be stated clearly with all governing material balances as constraints. It is an elegant approach that can lead to an improved process control strategy.

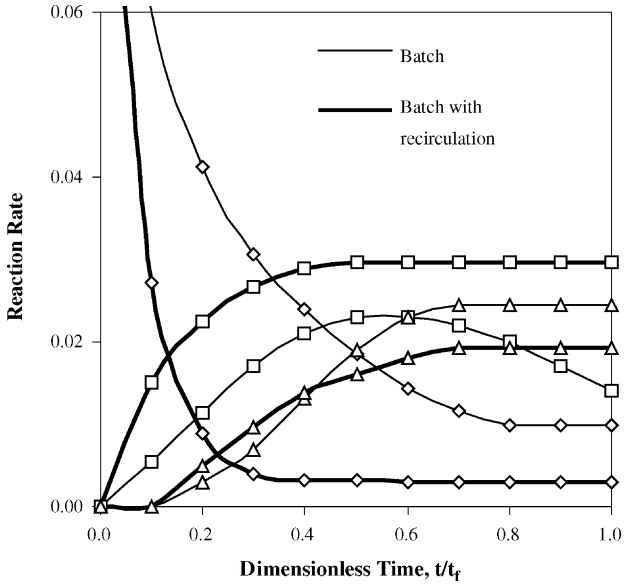

Fig. 6. The electrochemical reaction rate curve for the consecutive electrochemical reactions. (◊) Rate of disappearance of the reactant A, (□) rate of appearance and disappearance of the desired product B, (△) rate of appearance of the undesired product *E*.

5. Dynamic optimization of CSTER and PFER

The above development demonstrates how the optimal control theory can be applied to calculate the exact time-varying electrode potential in batch electrochemical reactors. It is also reasonable to look at the CSTER and PFER commonly known as electrochemical flow cells. The dynamic modeling of the former is comparatively simple as there is no spatial distribution of concentration within the reactor vessel as in the batch electrochemical reactors. But, in the latter case we need to account for the spatial concentration variation within the reactor from the inlet to the outlet in addition to the dynamics. These are considered as some realistic case for industrial scale reactors.

5.1. CSTER

Consider a typical CSTER as shown in Fig. 2c, the proposed formulation approach for CSTER is almost the same as batch processes. The material balance for species A can be written as:

$$V_R \frac{dC_A}{dt} = -k_{L_A} A_e (C_A - C_A^s) + qC_{A_0} - qC_A \tag{35a}$$

$$\frac{dC_A^s}{dt} = k_{L_A} a (C_A - C_A^s) - k_{fl_0} a e^{-\alpha_1 fE} C_A^s + k_{bl_0} a e^{-\beta_1 fE} C_B^s \tag{35b}$$

It can be noticed here that the terms describing flow of electrolyte is the only difference between this case and batch reactor without electrolyte recirculation. Likewise, the case of CSTER in series is also not much difficult to formulate a dynamic problem

since the number of ODEs governing a species behavior alone multiplies. For example, if two CSTERs are connected in series the component balance for A is

$$V_{R_1}\frac{dC_{A_1}}{dt} = -k_{L_A}A_e(C_{A_1} - C^s_{A_1}) + qC_{A_0} - qC_{A_1} \quad (36a)$$

$$\frac{dC^s_{A_1}}{dt} = k_{L_A}a(C_{A_1} - C^s_{A_1}) - k_{fl_0}ae^{-\alpha_1 fE}C^s_{A_1} + k_{bl_0}ae^{-\beta_1 fE}C^s_{B_1} \quad (36b)$$

$$V_{R_2}\frac{dC_{A_2}}{dt} = -k_{L_A}A_e(C_{A_2} - C^s_{A_2}) + qC_{A_1} - qC_{A_2} \quad (36c)$$

$$\frac{dC^s_{A_2}}{dt} = k_{L_A}a(C_{A_2} - C^s_{A_2}) - k_{fl_0}ae^{-\alpha_1 fE}C^s_{A_2} + k_{bl_0}ae^{-\beta_1 fE}C^s_{B_2} \quad (36d)$$

It is also possible to get the final converged trajectories of state, adjoint and control variables by following the same computation procedure. But, it may be needed to alter the default properties of the ODEs solver performance according to the degree of difficulty and errors reports or stiffness if any.

5.2. PFER

The system under discussion is depicted in Fig. 2d. A mass balance for component A on a length element δ_x of the reactor at any time $t>0$, noting that in this problem formulation the concentration is a function of both position and time, gives the following partial differential equation

$$\frac{\partial C_A}{\partial t} + U\frac{\partial C_A}{\partial x} = -k_{L_A}a(C_A - C^s_A) \quad (37a)$$

$$\frac{\partial C^s_A}{\partial t} + U\frac{\partial C^s_A}{\partial x} = k_{L_A}a(C_A - C^s_A) - k_{fl_0}ae^{-\alpha_1 fE}C^s_A + k_{bl_0}ae^{-\beta_1 fE}C^s_B \quad (37b)$$

where U is the average velocity of the electrolyte and 'a' is the specific electrode area. The PFR behavior can be approximated well by discretisation using orthogonal collocation. Such a discretised model shows good accuracy because it is know that orthogonal collocation preserves observability. Therefore, this method is a suitable approach for the problem at hand. Alternately, Maple's pdsolve command can also enable the solution. The pdsolve command currently recognizes a certain number of PDE families that can be solved by using standard methods. When the given PDE belongs to an unrecognized family, pdsolve uses a heuristic algorithm that attempts separation of variables based on the specific structure of the PDE. But, the use of pdsolve/numeric with these methods is restricted to a single parabolic/hyperbolic linear PDE that is first orders in time. The resultant partial differential equations may be solved rigorously or approximately, by assuming that the transient concentration changes that occur when the potential varies are negligible as followed by Bakshi and Fedkiw [1].

6. Conclusion

A dynamic model of the batch electrochemical reactors with and without electrolytic recirculation was designed using the existing model equations. It is based on the dynamics in the surface concentration of various reacting species and also the double layer charging process. Thus, the scope of the work is restricted far from the pseudocapacitance as it does not have a major role in electrochemical synthesis. In this fashion, the presented approach takes account of both Faradaic and non-Faradaic processes in the statement of dynamic optimization problem. The model was used for the dynamic optimal control of batch electrochemical reactors for industrially useful consecutive electrochemical reactions. In this the primary goal was to move toward a maximum concentration of the desired product, as high as possible for a given reactor and a secondary objective was to realize the extent possible concentration of the desired product using electrolyte recirculation.

The formulation achieved in this paper encompasses not only the polarizable and non-polarizable limits but also for the various batch electrochemical reactors so that it is possible to deduce from simple kinetic expressions the results of almost all reaction–reactor system of interest. Besides finding the optimal control policy, this paper has discussed few other aspects related to the methodology of dynamic optimization in continuous flow electrochemical reactors.

Acknowledgements

Fellowship support to Vijayasekaran Boovaragavan, jointly from the Council of Scientific and Industrial Research, New Delhi – India & Central Electrochemical Research Institute, Karaikudi – India is gratefully acknowledged.

References

[1] R. Bakshi, P.S. Fedkiw, J. Appl. Electrochem. 23 (1993) 715–727.
[2] B. Vijayasekaran, C. Ahmed Basha, N. Balasubramanian, Chem. Biochem. Eng. Q. 18 (2004) 359–366.
[3] F. Fournier, M.A. Latifi, G. Valentin, Chem. Eng. Sci. 54 (1999) 2707–2714.
[4] X.G. Zhou, X.S. Zhang, X. Wang, Y.C. Dai, W.K. Yuan, Chem. Eng. Sci. 56 (2001) 1485–1490.
[5] V. Costanza, Chem. Eng. Sci. 60 (2005) 3703–3713.
[6] B. Vijayasekaran, C. Ahmed Basha, Electrochim. Acta 51 (2005) 200–207.
[7] B.E. Conway, Electrochemical Supercapacitors Scientific Fundamentals and Technological Applications, Kluwer Academic/Plenum Publishers, New York, 1999.
[8] L.S. Pontryagin, V. Boltianski, R. Gamkrelidze, E. Michtchenko, The Mathematical Theory of Optimal Processes, Pergamon Press, New York, 1964.
[9] K. Jayaraman, C. Ahmed Basha, Electroorganic synthesis engineering, in: L.K. Doraiswamy (Ed.), Organic Synthesis Engineering, Oxford University Press, London, 2001.